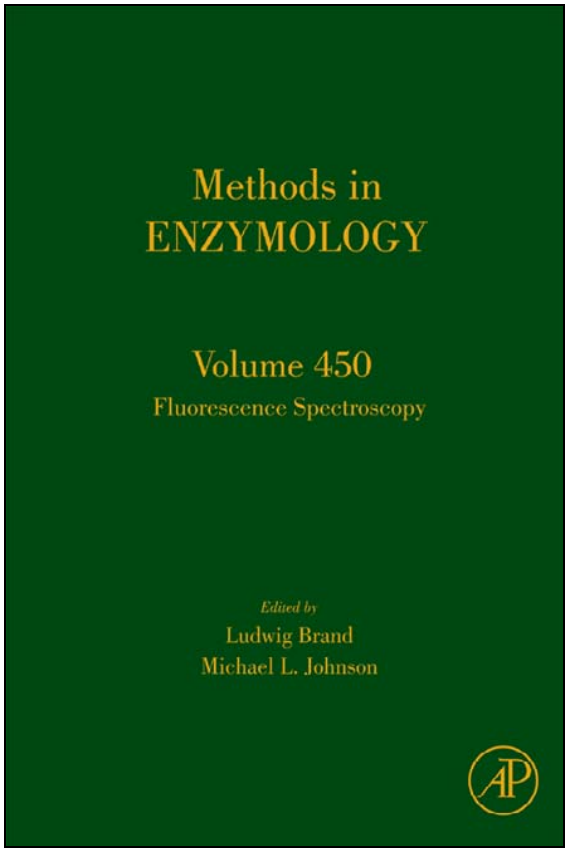

From: Mary E. Hawkins, Fluorescent Pteridine Probes for Nucleic Acid Analysis.
In Ludwig Brand and Michael L. Johnson, editors: Methods in Enzymology,
Vol. 450, Burlington: Academic Press, 2008, pp. 201-231.
ISBN: 978-0-12-374586-6

CHAPTER TEN

Fluorescent Pteridine Probes for Nucleic Acid Analysis

Mary E. Hawkins

Contents

Abstract

This chapter is focused on the fluorescent pteridine guanine analogs, 3MI and 6MI and on the pteridine adenine analog, 6MAP. A brief overview of commonly

National Institutes of Health, National Cancer Institute, Bethesda, MD 20892

Methods in Enzymology, Volume 450
ISSN 0076-6879, DOI: 10.1016/S0076-6879(08)03410-1

used methods to fluorescently label oligonucleotides reveals the role the pteridines play in the extensive variety of available probes. We describe the fluorescence characteristics of the pteridine probes as monomers and incorporated into DNA and review a variety of applications including changes in fluorescence intensity, anisotropies, time resolved studies, two photon excitation and single molecule detection.

1. Introduction

As we begin to tap into the vast potential for biochemical applications using sequences of DNA as probes and binding ligands, it will be very useful to understand the structure of these molecules and how a specific sequence of DNA can affect its function. It is clear that each specific sequence contributes to the features of a given locus in terms of flexibility or rigidity and consequently its association with other molecules. The overall function of DNA is dependent on these characteristics as it conveys the information needed for many vital processes in the cell. Subtle variations contribute to interactions between DNA and other factors, made even more complex by constantly changing conditions in response to alterations in the environment. They are all keys to the function of the DNA.

Fluorescence techniques are a natural choice to study these subtle variations because they provide information on the status of the DNA through measurement of fluorescence intensity, spectral shifts, lifetimes, steady-state anisotropies, and time-resolved anisotropies. It would be ideal to use the inherent fluorescence of DNA to study its structure and flexibility in a totally unaltered state, without introducing external probes of any kind. Although the very low fluorescence quantum yields of the native bases make it very challenging to do this, Georghiou *et al.* (1996) have used thymine fluorescence in poly(dA)–poly(dT) and in a dA–dT 20-mer in a structural study. This work reveals some features of the natural status of these bases in solution, the first to examine the movement of sequences using time-resolved intrinsic fluorescence anisotropy. It also provides us with an unadulterated look at the native features of the DNA for the sequences they studied. For most studies, however, the limitations that result from the extremely low yields of the native bases require that we find other ways to analyze these systems.

One way to achieve enhanced fluorescence labeling of DNA is to add an extrinsic fluorescent molecule to the structure. The introduction of any non-native molecule will have an impact on the structure through changes in the electronic field in its immediate environment. Some probes will have less negative impact than others simply because of their chemical structures. On the grosser level, we can assess the impact of a probe's structure on a sequence by measuring the melting temperature (T_m) of the duplex with

and without the probe present. Similar T_m measurements lead us to assume that at least the tertiary structure likely is intact. On a more subtle level, however, any change in the chemical nature of a sequence changes its character enough to potentially modify recognition by interacting molecules such as a highly selective enzyme. There are many systems that will tolerate addition of a fluorescent probe through incorporation, tagging, or intercalation, however, care should be used in designing the study and the proper controls must be carefully considered.

There are several ways to provide DNA with fluorescence. One is through saturation of the DNA with an intercalating agent. This method allows a view of the global status of the entire molecule as the probe distributes itself throughout the entire sequence. One example of the intercalation method uses ethidium bromide as a probe which naturally stacks between the bases of the sequence. Global dynamics of sequences have been studied using this technique. For a review, see Schurr and Fujimoto (1988). As with any extrinsic labeling system, there can be unwanted effects introduced by these fluorophores. Intercalating agents have been found to cause distinct changes in molecular elasticity and can extend and frequently partially unwind DNA double strands, so this must be considered when interpreting results (Sischka *et al.*, 2005). For many studies, however, this subtlety does not pose a problem and a great deal of valuable information can be obtained using this approach.

Another technique employs specific labeling with a linker-attached fluorescent molecule, usually at the terminal position of a sequence. This method has been used extensively and very successfully for labeling molecules. There are many studies using fluorophores which are attached to a sequence using carbon chain linkers of various lengths. Some of these linker-attached probes have been found to naturally have individual character that results in variations on the data (Unruh *et al.*, 2005b; Vamosi *et al.*, 1996). Fluorescein, a very commonly used probe, is often linked to the terminus of a sequence through a carbon linker. Hill and Royer (1997) have found that, in some cases, only about 15% of the linker-attached fluorescein undergoes rotation coupled to global motion of the DNA. In another study by Unruh *et al.* (2005a) the fluorescence properties of fluorescein, Texas Red, and Tetramethylrhodamine (Tamra) were compared in identical sequences. They determined that, of this group, Texas Red was the most reflective of global DNA motion. Experiments using fluorescein confirmed the findings of Hill and Royer (1997), and Tamra was found to be sensitive to the environmental which was seen to be a complicating factor for this type of measurement. Texas Red behaves uniquely because it appears to form an association with the bases of the sequence in the major groove. However, while this does much to stabilize it and permit measurement of global rotation of the DNA, it may actually interfere with the natural structure of the sequence and prevent native interactions in its vicinity.

The introduction of carbon linkers of varying lengths permits placement of the probe in areas where it might otherwise be structurally obtrusive.

A third method is through the incorporation of a nucleoside analog which is attached to the sequence through the same deoxyribose linkage as native DNA, preferably using automated DNA synthesis. This method has several advantages beyond the potential for visualization of the sequence. One is that the process of incorporation using automated DNA synthesis insures that the probe is covalently attached in every molecule of DNA. Also, there is no postsynthesis step for incorporation of the label, which can be very costly in terms of time and materials. The placement of the probe in the sequence permits observance of local changes that occur as it reacts with other molecules. A well known probe of this type, the adenine analog, 2-amino purine (2-AP), has been used extensively in studies of DNA base stacking and base pairing. One study examines properties of the TATA sequence, important because it is a part of a sequence involved in transcription initiation (Rai *et al.*, 2003). Xu and others have focused heavily on defining the most fundamental interactions between 2-AP and its neighboring bases (Davis *et al.*, 2003; Xu and Sugiyama, 2006). The dynamics of DNA have been studied through fluorescence lifetime and anisotropy decay kinetic measurements in 2-AP-containing sequences (Larsen *et al.*, 2001; Lee *et al.*, 2007; Ramreddy *et al.*, 2007). There are also a number of studies using pyrrolocytosine as a cytosine analog (Berry *et al.*, 2004; Dash *et al.*, 2004; Hardman and Thompson, 2006; Liu and Martin, 2001). New probes are constantly being developed (for a review of fluorescent nucleotide analog probes, see Rist and Marino, 2002). A survey of these probes shows that in some instances, probes that are insensitive to the sequence environment are best, while in others, a probe that reports on the immediate environment is preferred. The wide selection that is becoming available makes it an interesting task to select one that best fits the needs of a given system.

In this chapter, we will describe the features of the pteridine nucleoside analogs. In terms of size and structure, the highly fluorescent pteridine analogs, 3MI, 6MI, and 6MAP, are similar to the native purines, guanine, and adenine. This allows the pteridine molecule to be substituted for a purine and incorporated into an oligonucleotide through a deoxyribose linkage (Fig. 10.1).

A resulting feature of this incorporation is that, within an oligonucleotide, the pteridine ring system is intimately associated with neighboring bases and reflects changes in these associations through changes in fluorescence (Hawkins, 2001, 2003). The pteridines are significantly quenched primarily through base stacking interactions (and to a lesser degree through base pairing) and the degree of quench is dependent on the sequence of the DNA in the vicinity of the probe. Because of the high quantum yields of the monomer forms (listed below) nanomolar concentrations of pteridine-containing oligonucleotides can be detected easily (Hawkins *et al.*, 1995).

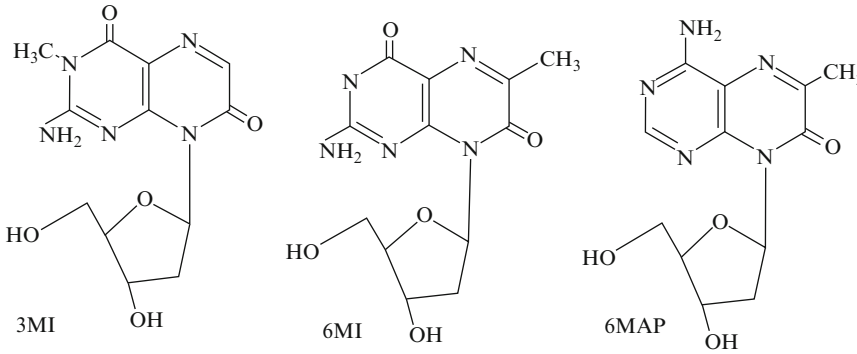

Figure 10.1 Chemical structures of 3MI, 6MI, and 6MAP.

One can engineer a pteridine-containing sequence that is surrounded with purines for a quenched signal or surrounded with pyrimidines for a brighter signal. The absorption and emission maxima of these probes are red shifted from the maxima of native DNA making them useful for DNA studies (Hawkins *et al.*, 1997).

Although it is clear that there are differences between the pteridine analogs and the corresponding native purines, the ability to position them as an integrated part of the DNA can provide a view of the subtle changes that accompany distortions in tertiary structure brought about by environmental changes. The associations between the incorporated pteridine analog and neighboring bases in a sequence provide information that is directly linked to structural changes in the DNA.

In this chapter, the properties of these pteridine nucleoside analogs are discussed to assist the researcher with the use of these probes. Procedures for synthesis and purification of pteridine-containing oligonucleotides are described. Examples are given of applications using fluorescence intensity changes, anisotropy, time-resolved studies, single molecule detection, and two-photon counting.

Note: The probes 3MI, 6MI, and 6MAP are commercially available through Fidelity Systems, Inc., Gaithersburg, MD (301) 527-0804; fsi1@fidelitysystems.com.

2. Pteridine Analog Characteristics

2.1. Intensity and spectral shifts

In the monomer form (unincorporated), the quantum yields for 3MI, 6MI, and 6MAP are 0.88, 0.70, and 0.39, respectively. In general, the adenine analog, 6MAP, is quenched more severely when incorporated

into an oligonucleotide than 3MI or 6MI, with quantum yields of 6MAP-containing single strands ranging from <0.01 to 0.04 depending on the neighboring sequence (Hawkins *et al.*, 2001). The single-stranded sequence-dependent variation in quantum yield for the guanine analog, 3MI, ranges from 0.03 to 0.29 (Hawkins *et al.*, 1995). Although 6MI seems to follow the same quenching patterns as 3MI, several notable exceptions have been found to show strong increases in fluorescence intensity upon duplex formation. The sequences involved in this anomaly are currently under investigation. In a recent study (described below) time-resolved anisotropy data suggests that 6MI may be mechanically coupled with neighboring bases to a larger extent than 3MI.

Variations in quenching patterns seen in pteridine probes incorporated into oligonucleotides have underscored the complexity of nucleic acid sequences. Driscoll *et al.* (1997) have determined that within an oligonucleotide, the distance between a 3MI molecule and the 5′-terminus does not seem to impact the fluorescence. A 3′-purine neighbor (especially adenine) appears to induce more quenching than a 5′-purine neighbor. The greatest quenching for 3MI is seen with adenines surrounding the probe and the lowest quench appears to occur when a probe is neighbored by thymine residues. The source of these effects was primarily attributed to *static* quenching mechanisms (or perhaps quasistatic, as studies of the first 50 ps have not been done).

Changes in pH have been shown to cause up to 10 nm shifts in the emission spectra of 6MI but this is seen to a lesser degree (~1–3 nm) in emission spectra of 3MI. Similarly spectral shifts are also seen when comparing 6MI monomer form to those of 6MI incorporated into single and double strands. Seibert *et al.* (2003) have compared the effects of pH on the ground state and lowest energy excited equilibria for 6,8-dimethylisoxanthopterin (6,8-DMI) an analog to 6MI in which the deoxyribose moiety is replaced with a methyl group (ruling out the possibility of interactions with the sugar). They found that the absorbance and fluorescence emission spectra are shifted to lower energies as the pH is increased and determined pKa values of 8.3 for absorbance and 8.5 for fluorescence. This group also demonstrated the involvement of the 3-position of the pteridine in this process by comparison of pH-dependent iodide ion quenching of 6,8,-DMI fluorescence with pH-independent absorption and fluorescence of 3,6,8-trimethylisoxanthopterin (an analog in which the 3-protonation site is blocked by a methyl group).

2.2. Stability

We have seen no evidence of degradation of the pteridine probes when exposed to ambient light. As one might expect, however, the phosphoramidite forms of the pteridines are vulnerable to hydrolysis in the same way

that the phosphoramidite forms of native bases are. To maintain pteridine phosphoramidites for long periods (years), we store them with desiccant in a −80 °C freezer.

Of these three probes, 3MI displays the greatest stability during fluorescence analysis. Using time-based acquisition (cuvette exposed to a spot-containing UV power <∼200 uW), we have monitored the fluorescence emission of a 3MI-containing oligonucleotide exposed at the excitation maximum for 2 h at 37 °C and observed no detectible change (loss) in the fluorescence intensity that could be an indication of photolysis (Hawkins *et al.*, 1995). Slight degradation of the fluorescence emission signals for 6MI- and 6MAP-containing oligonucleotides have been observed during time-based acquisition exposed at the excitation maximum at 37 °C. Three successive scans of oligonucleotides containing 6MI or 6MAP revealed no detectible loss in fluorescence intensity, however, which is an indication that short term exposure is less damaging (M. E. Hawkins, unpublished results).

All three of these pteridine probes have shown remarkable stability through the caustic conditions generated during automated DNA synthesis. As a quality control experiment, oligonucleotides containing each of the three probes were completely digested using P1 nuclease (*Penicillium citrinum*, Boehringer Mannheim Biochemica). The expectation for a stable probe would be that the fluorescence of the probe would be recovered by removing it from the quenched environment of the surrounding bases. For each probe, the ratio of the integral of the fluorescence emission spectrum of the oligonucleotide prior to the digestion to that of the corresponding digested product was equivalent to the ratio of the quantum yield of the probe-containing oligonucleotide to the quantum yield of the monomer form of the corresponding probe. This procedure is described in more detail in Section 4. The findings demonstrate that each probe remains intact and that the quench in signal originates from interactions with neighboring bases and not from degradation caused by exposure to chemicals during synthesis (for 6MAP, Hawkins *et al.*, 2001; for 3MI and 6MI, M. E. Hawkins, unpublished results).

2.3. Participation in base pairing

For 3MI, it is apparent that the methyl group in the 3-position should block formation of a hydrogen bond between the incorporated probe and cytosine. Melting temperatures (T_ms) of 3MI-containing oligonucleotides paired with a complementary strand (where 3MI is paired with cytosine) are similar to T_ms of a *single base pair mismatches* in the identical positions, and the degree of T_m depression is sequence dependent (Hawkins *et al.*, 1995).

6MI, however, displays evidence of base pairing with cytosine. The melting temperatures of 6MI-containing oligonucleotides paired to complementary strands are almost identical to those of control oligonucleotides of identical sequences. The emission maximum of 6MI also undergoes a

substantial shift (~10 nm to the red) at pH 8.0 as compared to that measured at pH 6.0. A comparable shift to the blue is seen when 6MI transitions from monomer to double strand at pH 7.2. These spectral shifts are suggestive of a change in status of the 3-position proton which is related to duplex formation.

6MAP also displays evidence of hydrogen bonding (with thymine) as determined by T_m measurements. To further investigate this, we measured the T_ms of 6MAP-containing strands paired with each of the four native bases: adenine, thymine, cytosine, and guanine, as a pairing partner in the complementary strand. The results clearly show that 6MAP pairing with thymine is the most stable (Hawkins *et al.*, 2001).

3. Procedures for Oligonucleotide Synthesis with Pteridine Analogs

3.1. Conservation of phosphoramidite

Automated DNA synthesis is a fairly routine procedure and because most of the reagents are relatively inexpensive, the standard synthesis protocols are quite liberal in use of reagents. There are some measures that can conserve the amount of pteridine phosphoramidite that is consumed during a synthesis. Most of our oligonucleotides are made using an ABI (Applied Biosystems, Foster City, CA) DNA synthesizer and the first point where the phosphoramidite may be unnecessarily lost is in the standard "bottle change" procedure. We dissolve the probe by hand using a freshly opened bottle of low water acetonitrile (ACN) at a ratio of 10 μl ACN per mg of probe phosphoramidite. For volumes of phosphoramidite solution under 1 ml, we place a smaller vial (12 × 32 mm P/N 5185-5821, Agilent Technologies, Wilmington, DE) containing the pteridine phosphoramidite inside one of the standard phosphoramidite bottles. The tubing must be trimmed for this application so that it just fits into the bottom of the inserted vial. After placing the phosphoramidite in the bottle, we use a modified "user program" to install the probe-containing vial on the synthesizer as advised by the company (ABI, Foster City, CA) which has a reduced phosphoramidite "flush to waste" time from "2" to "1 s."

We use 200 nM low volume columns (LV200, ABI, Foster City, CA) for any synthesis involving the probes. The low volume column has a frit that reduces the bed volume of the column thus requiring lower volumes of each reagent to accomplish each wash. The appropriate procedure to accommodate these columns on the synthesizer can be obtained from the company. The combination of these two modifications has increased the number of incorporations we can obtain from a given volume of phosphoramidite. We also avoid using the "Begin Procedure" when the pteridine

phosphoramidite is on the machine because this procedure involves flushing all lines with fresh reagents. Once the probe is on the machine sequences are made without delay so that the begin procedure is not needed. Other manufacturers of synthesizers may have suggestions of their own on how to reduce unnecessary losses of probe phosphoramidites.

3.2. Deprotection

Both 3MI and 6MAP are deprotected in the standard manner through incubation at 55 °C for 15 h in concentrated ammonium hydroxide.

The 6MI phosphoramidite has a paranitrophenyl group to block unwanted chemistry at the 3-position during DNA synthesis and because this group is not removed during standard deprotection using ammonium hydroxide (W. Pfleiderer, personal communication), additional steps must be taken to remove it. Oligonucleotides are not very soluble in 10% 1,8-diazabicyclo(5.4.0)undec-7-ene (DBU) in acetonitrile, the reagent required for this procedure, therefore, 6MI must be deblocked while the oligonucleotides are still attached to the column. When synthesizing 6MI-containing oligonucleotides select the ''manual end procedure'' and mark the identity of each sequence on the appropriate column. The oligonucleotides can be manually deprotected as described below.

After the synthesis is finished (and ready for ''manual end procedure'') set up each CPG column with an empty 3 ml luer lock syringe on each side removing the plunger from one syringe. Add 425 μl ACN to the plunger-less syringe (held upright) and pull it through to the opposing side using the plunger. Flush it through to the plunger-less side, add 75 μl DBU to the ACN and pull it through again. Insert the other plunger and use it to flush the samples back and forth at least three times. Put in a dark place at room temperature for 5 h. Flush the solution back and forth about once an hour.

After the incubation, pull the solution through and save it (eluate-1). Add 500 μl ACN to the column and flush it through several times. Add this wash to eluate-1 of each corresponding sample. Save the CPG columns for the next step. Monitoring the UV absorption of samples from each step has revealed that a substantial amount of oligonucleotide is released from the column during the deprotection steps. The eluate-1 samples may be evaluated to determine whether it is necessary to retrieve the oligonucleotide from them before continuing. If the optical density indicates the presence of oligonucleotide in these samples, evaporate the DBU/ACN mixture (eluate-1) using a Speed-vac. Perform an ethanol precipitation on the resulting DBU/ACN oily residue saving the pellet for the next step. Add 1 ml aliquots of NH_4OH to each sample (CPG column) using two syringes as described above, and allow them to stand for 1 h. Add the NH_4OH eluate (eluate-2) from each column to the corresponding DBU/ACN eluate-1 pellet, mix thoroughly and heat for 15 h at 55 °C. Speed vac and purify as usual.

3.3. Purification procedures

Oligonucleotides are purified by 20% denaturing polyacrylamide gel electrophoresis (19:1 acrylamide:bis). The oligonucleotide band, visualized using UV shadowing, is excised and extracted from the gel slice using an electroelution device (Schleicher & Schuell, Keene, NH). HPLC purification techniques may also be used. Following ethanol precipitation, the oligonucleotides are stored in a −80 °C freezer.

4. Characterization of Pteridine-Containing Sequences

The absorption of the pteridine at 330–350 nm should be detectable using a UV–VIS spectrophotometer and in a 20-mer should be about ten times less than the absorbance at 260 nm (representing mostly native bases). Naturally, this ratio will vary depending on the length and the sequence of the strand.

The quantum yield of the probe-containing oligonucleotide can be measured using quinine sulfate (QS) as a standard as previously described (Hawkins *et al.*, 1997).

When calculating the extinction coefficient of a probe-containing sequence, we use a method described by Eckstein (1991) with the extinction coefficients of 3MI as measured in methanol as log ϵ at 216 (254) 292 and 350 nm equal to 4.54 (3.69) 3.93 and 4.13, respectively (numbers in parentheses are for a shoulder) (W. Pfleiderer, personal communication).

The degree to which the presence of a probe may disrupt double-strand formation may be assessed from the melting temperature (T_m). We typically measure T_ms in 10 m*M* Tris at pH 7.5 in the presence of 10 m*M* NaCl.

One way to verify that the probe has not been degraded during the exposure to caustic chemicals during DNA synthesis is to totally digest the product strand and compare the fluorescence with that which would be expected for an equal amount of probe monomer. After determining the relative quantum yield of the sequence, set up a sample (100 μl volume) to digest with 3 Units of P1 Nuclease (*P. citrinum*, Boehringer Mannheim Biochemica, Germany). Scan the sample before digestion and then again after total digestion (overnight incubation). The ratio between the scans of the pre- and postdigest should approximately equal the ratio of the relative quantum yields of the sequence and the monomer. When this test was performed on oligonucleotides containing each of the three probes, the ratios obtained were almost identical to the values obtained from the starting sequence and the monomer form of the corresponding probe.

5. Applications

5.1. Using fluorescence intensity changes

Because the fluorescence properties of the incorporated pteridine nucleoside analogs are so heavily impacted by interactions with neighboring bases, any event that changes these associations can directly influence the fluorescence intensity of the probe. One of the simplest ways to monitor these interactions is through changes in fluorescence intensity.

The first experiment to take advantage of this effect using the pteridine probes was designed to measure a cleavage activity of the retrovirally coded protein, human immunodeficiency virus-1 (HIV-1) integrase (IN) (Hawkins *et al.*, 1995). This protein functions in a stepwise manner resulting in the integration of the HIV-1 genome into the host cell DNA with the first step being the cleavage of a specific dinucleotide from each end of the HIV genome. The pteridine probe, 3MI, was incorporated into a model substrate at a specific cleavage site known to be processed by the integrase. As the protein cleaves at the specific site, the probe is removed from the base stacked environment and the increases in fluorescence intensity can be monitored in real time. This is a distinct advantage over the previously used P-32-based assay using polyacrylamide gels and autoradiography for analysis.

Another example of using fluorescence intensity changes is the use of 3MI to assess the DNA-binding characteristics of the nonspecific multifunctional histone-like DNA-binding protein, HU, by Wojtuszewski *et al.* (2001) In this study, a change in fluorescence intensity was related to a change in base stacking due to local unwinding or bending of the DNA helix that occurs in the presence of HU concentrations below 4 μM. When measured as a function of HU concentration, the fluorescence intensity increase demonstrates saturable binding. Of the 3MI-containing strands examined, two 34-mers displayed a fluorescence intensity change while a 13-mer showed no change. This result was interpreted by the authors to indicate an absence of induced bending in the HU-binding interaction with the 13-mer. Binding stoichiometry, as determined by fluorescence intensity and confirmed by analytical ultracentrifugation, indicated that either the binding site size or the mode of binding is altered between the longer and shorter strands. The fluorescence intensity-based data was combined with changes in the anisotropy of the 3MI-containing oligonucleotides (discussed briefly below) to assess the binding characteristics.

Myers *et al.* (2003) have used 6MI-containing sequences to map specific binding between single-stranded DNA and unwinding protein (UP1), a subunit of heterogeneous ribonucleoprotein A1, a protein strongly involved in RNA processing. These researchers designed the 6MI-containing substrate sequences after examining the structure of UP1 bound to the

heterogeneous telomeric repeat sequence d(TTAGGG)$_n$ as determined by X-ray diffraction. They substituted 6MI for guanine in two different positions, TR2-6F where 6MI is expected to become unstacked when bound to protein, and TR2-11F, where it is expected to remain stacked when bound. X-ray diffraction studies of the 6MI-containing sequences complexed to UP1 demonstrated that the presence of 6MI in the sequences did not significantly change the tertiary structure of the complex. The changes in fluorescence intensity seen upon binding these sequences to the UP1, three- to fourfold for TR2-6F and 1.2-fold for TR2-11F, confirmed structural predictions based on the crystallographic data. The magnitude of change in fluorescence intensity seen with 6MI in the unstacking position, TR2-6F, permitted the determination of binding isotherms under tight-binding conditions with protein at 10 n*M*. These authors demonstrate the usefulness of 6MI as a probe for determination of equilibrium binding between protein and nucleic acids.

5.2. Fluorescence characterization of A-tracts using 6MAP

In a study by Augustyn *et al.* (2006), the fluorescence properties of the adenine nucleotide analog, 6MAP, have been investigated within the context of DNA "A-tracts," DNA sequences consisting of two or more adjacent adenine residues. When A-tracts are repeated in phase with the DNA helix, these sequences exhibit curvature or bending. Gel mobility measurements showed previously that A-tracts of six residues exhibit the maximum amount of curvature (Crothers and Shakked, 1999). The fluorescent analog, 6MAP, was substituted for adenine residues in five oligonucleotides both to asses the fluorescence properties of 6MAP in the context of these sequences and to probe the relative differences in structure of these sequences. The sequences were (see Table 10.1) characterized in both single- and double-stranded forms.

The fluorescence signal of 6MAP is quenched upon incorporation into a single strand by over 95% in all five oligonucleotides, relative to free monomer.

Table 10.1 Oligonucleotides containing 6MAP

Name	Sequence[a]	Φ_{rel} (SS)[b]	Φ_{rel} (duplex)[b]
A3-1	5′-CGCA**F**ATTTCGC-3′	0.017	0.013
A3-2	5′-CGCAA**F**TTTCGC-3′	0.036	0.019
T3-1	5′-CGCTTTA**F**ACGC-3′	0.022	0.012
T3-2	5′-CGCTTT**F**AACGC-3′	0.033	0.027
AT-1	5′-CGCAT**F**TATCGC-3′	0.039	0.015

[a] F denotes the position of the fluorophore in the oligonucleotide strand. For control sequences, F = A.
[b] Φ_{rel} represents quantum yields relative to that of the 6MAP monomer (0.39) as measured relative to quinine sulfate (Hawkins *et al.*, 2001).

The adjacent nucleotide neighbors strongly influence the degree of quenching, with the lowest quantum yields observed for the A3-1 and T3-1 oligonucleotides where 6MAP is situated between two adenine residues (Table 10.1). For the case of A3-2, T3-2, and AT-1 oligonucleotides, with at least one pyrimidine neighbor adjacent to 6MAP, the fluorescence intensity is not as quenched. In general, the emission maximum shifts seen upon incorporation into the single strand are relatively small.

Duplex formation further reduces 6MAP fluorescence intensity. The AT-1 oligonucleotide containing 6MAP has the largest relative quantum yield as a single-stranded molecule and experiences the greatest fluorescence quench upon duplex formation (62%). The A3-1 and T3-1 duplexes, in which 6MAP is situated between two adenines, have the lowest quantum yields in the single strand and the A3-1 duplex displays the least fluorescence quenching upon duplex formation. Nearest neighbor interactions are not sufficient to explain the relative quantum yields of the duplexes and undoubtedly, other factors, such as local structure of the duplex, have an impact. An interesting example of the effect of local structure can be seen in a comparison of T3-2 and A3-2 duplexes, where 6MAP is located in between adenine and thymine residues. In the single-stranded forms, the two dodecamers have similar fluorescence quantum yields; however, upon duplex formation the quantum yield of the A3-2 duplex decreases substantively compared to the T3-2 duplex. Since 6MAP has the same neighboring bases in both duplexes, the difference in quenching upon duplex formation most likely arises because of the change in orientation of the neighboring bases, AFT in A3-2 versus TFA in T3-2 (Table 10.1).

Duplex formation also results in a shift of peak emission to a shorter wavelength for each of the sequences studied. The A3-1 and AT-1 duplexes exhibit the largest shifts, −14 and −13 nm, respectively. Emission shifts appear to be more reflective of local nucleic acid duplex structure rather than local environment caused by neighboring residues (base stacking), since the A3-1 and T3-1 duplexes have the same neighboring residues and display quite different shifts; A3-1 (−14 nm) and T3-1 (−8 nm). Similarly, the A3-2 duplex, with 6MAP located at the 3′-end of the A-tract, exhibits the smallest shift in emission maximum, possibly reflecting local structure close to the probe.

Nearest neighbor interactions have a greater influence on the stability of duplexes containing 6MAP. Thermal melting temperatures (T_m) as measured by UV–VIS absorption spectroscopy reveal that 6MAP-containing sequences are destabilized by 2–5 °C as reported previously (Hawkins *et al.*, 2001). The greatest perturbations in stability ($\Delta\Delta H$ = 5.5 kcal/mol as determined from the UV melting curves) were observed for the A3-1 and T3-1 sequences, in which 6MAP was situated between two adenines. The smallest perturbation ($\Delta\Delta H$ = 2.5 kcal/mol) was detected for the AT-1 duplex, in which 6MAP is between two thymine residues.

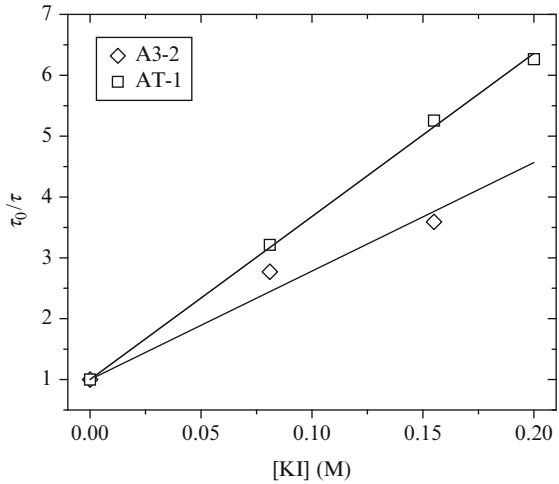

Figure 10.2 Stern–Volmer plot of the longest lived component for the A3-2 and AT-1 duplexes. Ksv = 18 mol per KI for the A3-2 duplex and 27 mol per KI for the AT-1 duplex. Measurements were performed in 0.0, 0.08, 0.15, and 0.20 M KI solutions with 5 m*M* $Na_2S_2O_4$ in a 10 m*M* Tris buffer at pH 7.4. KCl was added to maintain a constant ionic strength of 0.2 M.

The environment of the probe within different duplexes was investigated using KI quenching. A Lehrer analysis was used to analyze the steady-state fluorescence quenching behavior of KI on the dodecamers (Lakowicz, 1999). These data reveal that the fractional accessibility of 6MAP in all five duplexes is at least 83%. Time-resolved experiments indicate that the fluorescence behavior of 6MAP in the duplexes is relatively complex exhibiting at least two lifetime components; the longer component, 4.6 ns, similar to free 6MAP monomer (3.8 ns) (Hawkins *et al.*, 2001), and a shorter component of 0.4 ns. The 4.6 ns component is strongly affected by KI, while the 0.4 ns lifetime component remains relatively constant in the presence of increasing KI quencher (Fig. 10.2).

These studies indicate that 6MAP situated between two pyrimidines is the most accessible to quencher. Comparable quenching constants to those found for A3-2 were obtained for the other duplexes, in which 6MAP is adjacent to at least one purine residue, an indication that accessibility is reduced significantly even with one purine neighbor.

5.3. Temperature-dependent behavior of A-tract duplexes

6MAP fluorescence has also proven to be an effective means to site specifically probe A-tract structure and stability. Considerable spectroscopic and calorimetric evidence exists which suggests that A-tract duplexes undergo a

transition from a bent to a straight conformation with a midpoint of ~35 °C (Chan *et al.*, 1990, 1993; Mukerji and Williams, 2002; Park and Breslauer, 1991). This premelting transition is characteristic of duplexes containing A-tracts in a 5′- to 3′-orientation, as in A3-1 and A3-2, but not a 3′- to 5′-orientation, as in T3-1 and T3-2 (Park and Breslauer, 1991). We have monitored the fluorescence behavior of the single- and double-stranded oligonucleotides (shown in Table 10.1) as a function of increasing temperature. We observe that the fluorescence intensity of the monomer probes and the single-stranded oligonucleotides decrease relatively linearly as a function of temperature which is attributed to an increase in the relative efficiency of other processes such as internal conversion and vibrational relaxation.

The 6MAP-containing duplexes also exhibit emission maxima shifts as a function of increasing temperature. For each of the four duplexes at 80 °C, the emission maximum shifts to the same value (±1 nm) as that observed for the corresponding single-stranded oligonucleotide at 80 °C. This behavior is consistent with exposure of the 6MAP probe to solvent and an absence of stacking interactions at high temperature. The fluorescence intensity of the duplexes can also be monitored as a function of temperature. Since the fluorescence yield of the single-stranded oligonucleotides is greater than that of the duplexes (Table 10.1), melting of the duplexes leads to an initial decrease in fluorescence intensity followed by an increase in intensity. A ratio of the fluorescence intensity of the duplex and the single-stranded oligonucleotides yields a sigmoidal curve that is characteristic of the cooperative DNA melting process (Fig. 10.3).

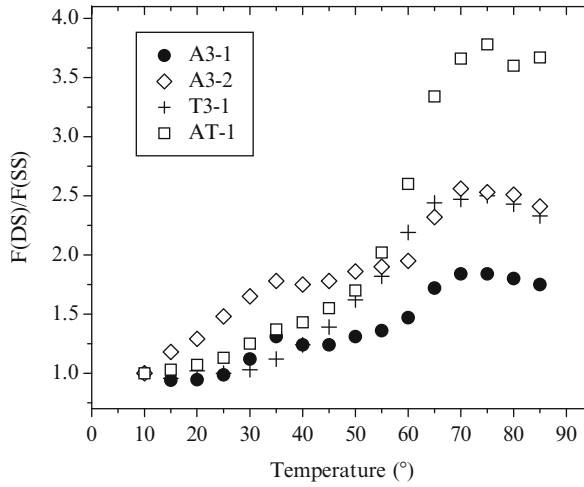

Figure 10.3 Fluorescence of the A3-1, A3-2, T3-1, and AT-1 duplexes as a function of temperature. The fluorescence of the duplex is ratioed against that of the single strand. Measurements were performed in a 0.5 *M* NaCl, 10 m*M* Tris buffer at pH 7.4.

By using a ratio of the data, the decrease in fluorescence intensity as a consequence of increased temperature is suppressed. Similar profiles are obtained if the ratio is done with the monomer instead of the single-stranded oligonucleotide. The maximum shift in peak emission occurs at the same temperature as the T_m as measured from the fluorescence intensity change.

A premelting transition is observed in the melting profiles of the A3-1 (•) and A3-2 (◇), but not the T3-1 (+) duplexes (Fig. 10.3). The influence of 6MAP on melting behavior cannot be ignored, however, this influence should also be seen in the control duplexes T3-1 and AT-1, which show no evidence of a premelting transition. In this study, 6MAP is used to investigate specific sites in DNA duplexes of identical base composition, but different sequence, and the fluorescence signals observed clearly reveal subtle differences in DNA structure and that the locus of the premelting transition is in the A-tract.

5.4. Bulge hybridization

In many cases, a quench in fluorescence intensity is seen when a pteridine-containing oligonucleotide is annealed to a complementary strand, however, the changes are usually small and reported through a loss in fluorescence intensity (Hawkins *et al.*, 1997). We have developed a technique that reports on hybridization of sequences in solution by displaying substantial increases in fluorescence intensity (Hawkins and Balis, 2004).

The quench in fluorescence intensity seen with pteridines incorporated into a single strand has been attributed mostly to base stacking interactions. When a 3MI-containing oligonucleotide is annealed to a complementary strand that does not contain a base pairing partner for the fluorophore, the probe can be pushed out of base stacking interactions resulting in increased fluorescence intensity. This sequence-specific technique can result in increases in fluorescence intensity of up to 27-fold (Fig. 10.4).

Almost all sequences we have tested display some increase in fluorescence intensity upon hybridization, however, the largest increases are seen with two adenines on each side of 3MI. A specific sequence containing one, two, or three 3MI probes per strand was tested to determine the optimum condition for that sequence. Each was also tested for potential disruption of annealing from the probes by analyzing T_ms as compared to the control (71.4 °C). It was found that with one probe per strand there was an eightfold increase and a T_m of 70.4 °C, for two it was eightfold and 68.6 °C, for three it was 10-fold and 66.6 °C and for four it was 10-fold and 63.6 °C. In another experiment we examined the optimum length of strand for bulge formation. The results are strongly dependent on annealing conditions including buffer, salt, and overall sequence. In the one sequence that was tested for this, using 10 m*M* Tris, pH 7.5 in 10 m*M* NaCl, we found that the greatest increases were in strands of at least 21 bases in length.

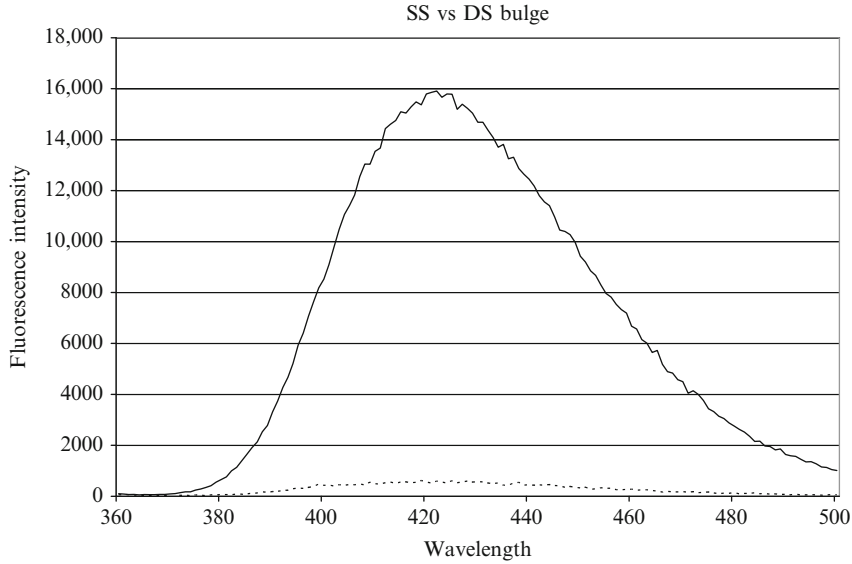

Figure 10.4 Fluorescence emission scans of the single-stranded 3MI-containing oligonucleotide, 5′-cct cta aga ggt gta aFa atg tgg aga atc tcc-3′, as a single strand (dashed line) and annealed to its complementary strand (5′-gga gat tct cca cat ttt aca cct ctt aga gg-3′) which does not contain a base pairing partner for 3MI (solid line). Samples were measured at 25 °C in the presence of 10 m*M* NaCl.

Results will most likely differ depending on the neighbors for the probe, overall sequence, and the distance of the probe from a 3′- or 5′-terminus and should be determined for each sequence experimentally. While this study was done with 3MI as the probe, selected sequences containing 6MI or 6MAP have been found to behave in a similar manner (M. E. Hawkins, unpublished results).

The usefulness of this application has been demonstrated by measuring the presence of positive polymerase chain reaction (PCR) product for HIV-1. The probe in this study (5′-taa ata aFaa tag taaF gaa tgt ata gcc cta cc-3′ with F = 3MI) is complementary to a region in the 115 bp PCR product defined by the HIV-1 *gag* primers SK38/SK39 (Ou *et al.*, 1988). Reactions contained varying amounts of template from the plasmid, pSum9, generated from a full-length HIV molecular clone (Tanaka *et al.*, 1997). The 3MI-containing sequence was present in the reaction mixture during the amplification process and results were compared to a sample identical in all components and handling except that it contained no template. Experiments were performed in duplicate and repeated at least three times. Increases in fluorescence intensity were proportional to the amount of template added and resulted in signal changes of up to three- to fourfold (Fig. 10.5).

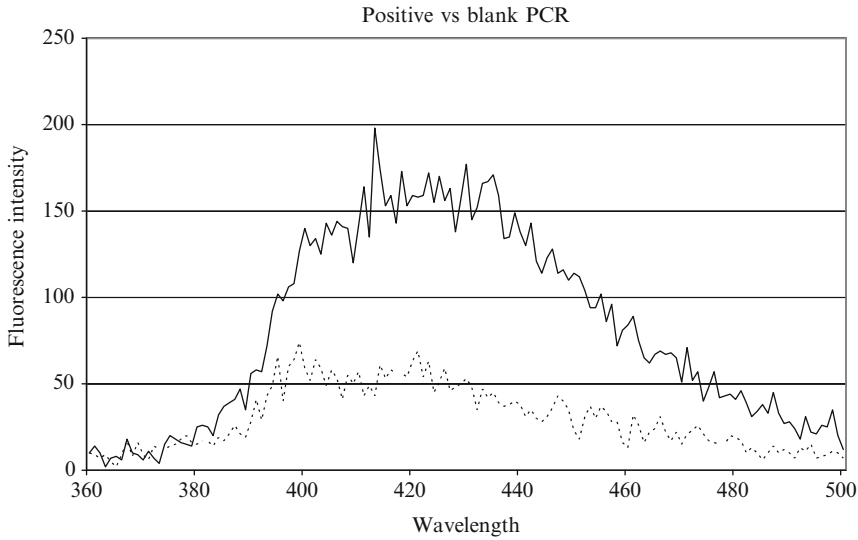

Figure 10.5 Fluorescence emission scans from positive (solid line) and blank (dashed line). The positive sample contained 2.5×10^6 copies of the template. Both samples contained identical concentrations of all components for the amplification including 25.6 n*M* of the 3MI-containing PCR probe and were subjected to identical amplification procedures with the negative control containing no template. All samples were measured at 25 °C.

A 3MI-containing strand that was not complementary to the PCR product was used as a negative control and showed no increase in fluorescence intensity after amplification. Blocking the probe to prevent it from functioning as a primer would permit the use of higher concentrations of the probe without interfering with the primers. Monitoring the results in real time would also improve this technique.

The results of the bulge hybridization study revealed that the optimum sequence for obtaining a strong increase in fluorescence intensity upon binding would include the probe having two adenines on each side, containing one or two probes in a sequence at least 21 bases long. The design of probe-containing sequences for this application should include a test of the probe's performance under conditions of the system under study.

5.5. Anisotropies of pteridine-containing sequences to examine protein binding

Anisotropies of 3MI-containing sequences were first used to probe protein/DNA binding by Wojtuszewski *et al.* (2001) in a study of HU protein (described in Section 5.1). In this study, the authors found that the

anisotropy of a 3MI-containing 13-mer ranged from 0.04 to 0.076 in the transition from unbound DNA to HU-bound DNA while the corresponding anisotropy of a 3MI-containing 34-mer sequence went from 0.12 to 0.22 during the same transition. Based on these results combined with results from observation of changes in fluorescence intensity and data from analytical ultracentrifugation, the authors propose a model for binding stoichiometry that is supportive of three HU molecules binding to the 34 bp sequence (accompanied by bending of the DNA) and two HU molecules binding to the 13 bp duplex. When changes in fluorescence intensity are observed upon binding, it is likely that changes in lifetime that accompany protein binding will result in the observation of a lesser steady-state anisotropy change. Fluorescence intensity changes are likely to occur when pteridines are used in binding studies because of the probe's association with its environment and this must be considered when interpreting results as these authors have done.

Nucleoside analog probes may provide some advantages over linker-attached probes in the analysis of anisotropy data. The presence of a linker arm can potentially complicate the interpretation of results. An example of this is stated in a study by Hill and Royer (1997), where it was determined that 85% of the signal change seen upon binding a fluorescein probe attached through linker chemistry was due to rotational motions associated with the linker, *not* due to the global motions of the DNA.

5.6. Lifetimes, steady-state and time-resolved anisotropies of 3MI- and 6MI-containing sequences

In an ongoing study by Wojtuszewski *et al.*, we have examined the fluorescence characteristics of oligonucleotides containing each of the two probes, 3MI and 6MI. The sequence 5′-act aFa gat ccc tca gac cct ttt agt cag t*F*t gga-3′ was used as a model for this analysis. 3MI or 6MI was incorporated into one of the positions shown for each sequence and analyzed in a single or double-stranded environment. In this study the sequence containing the aFa (near the 5′-terminus) environment is expected to be more quenched and the sequence containing the tFt environment is expected to be less quenched.

Measured steady-state anisotropies of 3MI-containing single strands were 0.088 and 0.093 in the less quenched and more quenched environments, respectively. The variation between measurements (averaged from at least three samples each) for duplex environment with 3MI were 0.072 and 0.054, respectively. For 6MI the variation between less quenched and more quenched was 0.103 and 0.154 for the single and 0.154 and 0.206 for the duplex, respectively. Steady-state anisotropy measurements are the result of an average of stacked and partially stacked states within each of these structures. An interesting finding in the 6MI-containing set is that in the

Table 10.2 Lifetimes

	α_1	τ_1 (ns)	α_2	τ_2 (ns)	α_3	τ_3 (ns)	$\langle\tau\rangle$ (ns)	τ_m (ns)
3MI ss	21	1.03	28	4.28	51	0.15	1.49	3.60
3MI ds	10	1.25	14	5.72	75	0.14	1.04	4.61
3MI	2	3.54	98	6.58			6.55	6.52
6MI ss	19	1.00	10	4.7	71	0.21	0.81	3.00
6MI ds	17	0.93	5	5.59	78	0.34	0.70	2.56
6MI	20	5.45	80	6.58			6.39	6.35

Abbreviations: τ_i, lifetime for each component of a multiexponential model; α_i, pre-exponential for each component of a multiexponential model; $\langle\tau\rangle$, species-concentration-weighted lifetime; τ_m, *intensity-weighted lifetime*.

duplex form of the less quenched sequence, the quantum yield of the probe almost doubles (compared to the single strand). This is different from what we would expect and very different from the behavior of 3MI-containing sequences.

The lifetimes, mean lifetimes, and amplitudes for the identical more quenched 36-mer sequences (aFa) defined above are shown in Table 10.2.

Changes in intensity-weighted lifetime (τ_m) between the single and double strands of these two probes in their single- and double-stranded forms may provide some insight into the type of quench the probes are experiencing within these structures. The amplitude of very short lifetimes (0.14–0.34 ns) is combined with the quantum yield defect; together these are taken to represent the portion of total fluorescence that is quasistatically quenched by the neighboring bases through base stacking interactions. Thus, the 3MI-containing sequences are 51–75% quasistatically quenched. The τ_1 and τ_2 values, in contrast, represent the monomer-like behavior that is representative of the probe in a more solvent exposed environment. These values are, of course, an average of multiple unstacked and partially unstacked populations subject to some forms of dynamic quenching. The fact that the changes in lifetime are disproportionate to changes in fluorescence intensity seen during these transitions (not shown) is an indication that the factors contributing to the changes are comprised of a combination of dynamic and static quenching interactions. We have not tested associative models for these data, however, the fact that the changes in lifetime are modest indicates that the nonassociative models will yield similar results. It may be difficult to do associative analysis when the lifetimes of the two different states (in this case, single- and double-stranded) are so similar (Brand *et al.*, 1984; Davenport *et al.*, 1986). In general, it might be expected that a double-stranded sequence (as compared to a single strand) would afford fewer degrees of rotational freedom for an incorporated probe. The results for 6MI (requiring fewer components to obtain a good fit) appear to

Table 10.3 Time-resolved anisotropy measurements

	β_1	φ_1 (ns)	β_2	φ_2 (ns)	β_3	φ_3 (ns)	χ^2
ss3MI	0.167	0.637	0.057	2.43			1.95
ds3MI	0.10	1.29	0.35	0.11	(−0.15)	(0.003)	2.04
ss6MI	0.071	6.66	0.23	0.857			1.12
ds6MI	0.32	2.09	(0.214)	(0.032)	(0.05)	(0.004)	1.17

Abbreviations: β_i, pre-exponentials for each component of a multiexponential model; φ_i, rotational correlation times for each component of a multiexponential model; χ^2 is derived from a model to assess goodness of fit.

confirm this. For 3MI, lifetime results agree with results from the steady-state anisotropies revealing similarity between single- and double-strand configurations. This suggests that 3MI does not participate in hydrogen bonding with cytosine, as expected from the steric hindrance from the 3-methyl moiety.

Table 10.3 shows the results from the time-resolved anisotropy studies.

The 3MI-containing single strand displays much shorter rotational correlation times (0.64 and 2.43 ns) compared to those of the 6MI-containing single strand (6.66 and 0.86 ns). Based on the lack of a long correlation time component, the motion of 3MI appears to be poorly coupled to the overall motion of the DNA. Although we are quite certain that these results are sequence dependent, it seems that even in a single strand, 3MI's association with neighboring bases may be significantly weaker than those of 6MI.

Until now, we have based the assessment of probe positioning in a double strand totally on measurements of melting temperatures of probe-containing sequences (Hawkins *et al.*, 1997). The current results suggest that 6MI may be more stably associated with, and consequently more accurately reflect the global motion of DNA than 3MI. Further studies are now in progress to explore the dependence of these results on the identity of neighboring bases.

5.7. Probing the hairpin structure of an aptamer using 6MI

In an ongoing study, Hawkins *et al.* are using the 37-base DNA aptamer, D17.4, as a model system for investigations of structure using 6MI. This aptamer which has the sequence of (5′-ggggcacgtttatccgtccctcc-tagtggcgtgcccc-3′) is known to bind with nM affinity to human immunoglobulin E, IgE, in a highly specific manner and is predicted to have the structural elements of a stem, a single base bulge and a hairpin loop (Gokulrangan *et al.*, 2005; Wiegand *et al.*, 1996). A comparison of steady-state anisotropies of 3MI and 6MI, each of which is directly incorporated into the 5′-end through a deoxyribose linkage, with that of Texas red, attached to the 5′-terminus of the sequence through a 21-carbon linker has

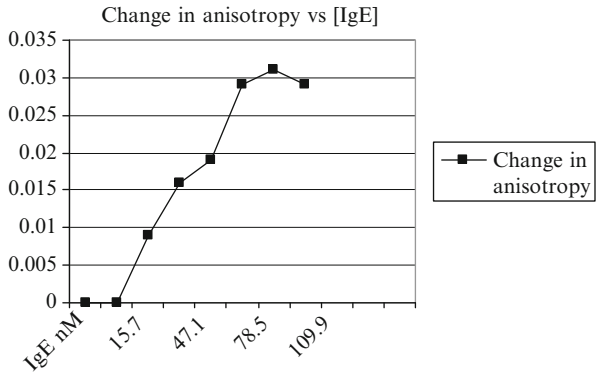

Figure 10.6 The increase in anisotropy of AP33 reveals a direct response to increasing concentrations of IgE protein. AP9 (6MI substituted for the 9th guanine) and AP16 (6MI substituted for the 16th guanine) showed no anisotropy changes in response to added IgE most likely because of the selectivity of binding in the area of the loop where they are located.

revealed large differences dependent on the nature of the probe. Steady-state anisotropies of sequences labeled at the 5′-terminal position with 3MI and 6MI were 0.013 and 0.018, respectively, while the sequence labeled at the same site with Texas Red was 0.16. Results for the pteridines suggest rapid segmental motion, in this case not attributable to a linker and so therefore most likely a feature of this site. For Texas Red, the linker attachment is thought to permit most of the probe to ''fold back'' and associate with the rigid annealed sequence, providing anisotropy values determined mostly by the molecule's overall motion (Unruh *et al.*, 2005a). Others have explained the rapid motion seen in linker-attached probes at the terminal position of a sequence to the motion of the linker. 6MI and 3MI are attached to the sequence through the native deoxyribose linkage, therefore, this rapid motion is likely associated with fraying of the duplex ends. 6MI was also incorporated into sites within the aptamer in either the stem or loop environments of the molecule. Steady-state anisotropies of 6MI at these positions range from 0.14 to 0.03 depending on the location. The position most reflective of ''global motion'' appears to be in the stem of the sequence where the 6MI probe is substituted for the guanine located 33 bases from the 5′-end (AP33). The same sequence was also used in a binding study with IgE (results shown in Fig. 10.6).

Time-resolved studies should reveal whether these steady-state differences represent actual changes in the motion of the DNA aptamer, or if they are the result of concomitant changes in lifetimes and fluorescence intensities.

5.8. Two-photon excitation of 6MAP

The utility of fluorescent base analogs is their ability to act as dynamic reporters of changes in DNA conformation. 6MAP is similar to 2-Ap (Nordlund *et al.*, 1989) in that it is an effective reporter of base stacking. It has a significantly larger Stokes shifted emission compared to 2-Ap (100 vs 50 nm) making it useful for certain applications involving microscopy and fluorescence resonance energy transfer. A problem with both analogs is that the lowest lying electronic transition of significant oscillator strength is in the near-UV (~317 nm for 2-Ap and 326 nm for 6MAP). Since many molecules absorb in this region it will be difficult to utilize single molecule techniques due to autofluorescence from buffer components, etc.

Two-photon excitation (TPE) has been used to ameliorate the problem of out of focus autofluorescence and is now widely implemented for biological imaging. TPE is a nonlinear process where two photons must be available simultaneously for efficient excitation. This implies high light intensities, which can be achieved by focusing short pulse mode-locked laser light. TPE is, therefore, only efficient in the focal volume of the laser. If a sufficiently short focal length optical system is used then excitation can be isolated to a very small volume, typically 1 μm^3. Since the exciting light has double the wavelength of the transition (i.e., 652 vs 326 nm) there will be no extraneous absorption outside of this focal volume and therefore a large reduction in the autofluorescence due to solvent components or other endogenous fluorophores. Secondly, due to the small focal volume and relatively large penetration depth of long wavelength light compared to near-UV excitation it is possible to selectively excite and image structures with a resolution on the order of the focal volume as well as perform studies on single molecules. Drawbacks to this approach have to do with the inefficiency of TPE compared to one-photon excitation and the difficulties associated with quantitation of the signal intensity. Stanley *et al.* (2005) have used TPE to assess whether 6MAP emits two-photon-induced fluorescence (TPIF) and their preliminary data suggests that it will make a useful TPE probe.

TPIF spectra were obtained from 6MAP monomer solutions using a nonlinear optical parametric amplifier (NOPA) as an excitation source. A full description of this work will be presented elsewhere. Samples of 6MAP (50–240 μM) were dissolved in Tris buffer, pH 7.4, 5% glycerol, and placed in a cuvette having a 1 cm excitation path length and a 0.2 cm emission path length. Solutions were stirred to avoid saturation and photobleaching effects. It should be noted that 6MAP has no one-photon absorption above about 380 nm. The energy of the *ca.* 300 fs pulse centered around 690 nm (1 kHz repetition rate) was controlled using a variable neutral density filter and measured with a sensitive joulemeter. This

wavelength was chosen because of the availability of two-photon cross-section values for standard compounds such as fluorescein and rhodamine dyes (Xu and Webb, 1996). The maximum useable energy was limited by continuum generation in the solvent (about 2.2 μJ/pulse) and depended on the choice of focusing optics (5 cm focal length) as well as the pulse energy. Fluorescence from the focal volume was collected using a 5 cm lens, filtered to remove residual excitation light, and focused into a spectrograph with a cooled low noise CCD detector.

TPE of solutions of 6MAP with 690 nm light generated blue emission visible to the naked eye, which emanated from the focus of the excitation beam. TPIF spectra were obtained for both 6MAP and QS (Heller *et al.*, 1974). QS was used as a standard for correcting the spectral responsivity of the measuring apparatus (for both one- and two-photon emission data).

When solutions of 6MAP are excited with focused ultrafast laser pulses from 614 to 700 nm blue fluorescence can be seen emanating from the focal point in the sample cuvette. For reference the one-photon absorption spectrum of 6MAP in buffer (ð) is shown in Fig. 10.6.

The absorption spectrum has structure with the largest extinction at about 330 nm and a prominent shoulder at 294 nm. The two-photon-induced fluorescence spectrum (TPIF) of a 240 μM solution of 6MAP in 50 mM Tris (pH 7.4) with 5% glycerol with excitation at 690 nm is shown in Fig. 10.6. The spectrum was corrected for the spectral responsivity of the instrument using QS. For comparison a one-photon-induced fluorescence (OPIF) emission spectrum of 6MAP at 20 μM concentration in the same buffer using 345 nm excitation is also shown, taken on a conventional fluorimeter with the same resolution whose spectral responsivity has been corrected using QS as indicated above.

Stanley and Yang performed a power dependence study to verify that the emission was due to TPE. The results of this study are shown in Fig. 10.7, where the logarithm of the TPIF is plotted versus the logarithm of the excitation power. A linear fit gave a slope of 2.0 ± 0.1 which is the value expected for a two-photon process. This value was obtained over the concentration range given above, indicating that dimerization does not affect the measured two-photon cross section:

$$\delta_{\mathrm{TPE}}^{\mathrm{6MAP}}(\lambda) = \frac{\delta_{\mathrm{TPE}}^{\mathrm{S}} \Phi_{\mathrm{f}}^{\mathrm{S}} [S] \langle F(t) \rangle_{\mathrm{6MAP}}}{\Phi_{\mathrm{f}}^{\mathrm{6MAP}} [\mathrm{6MAP}] \langle F(t) \rangle_{\mathrm{S}}}. \tag{10.1}$$

To measure the two-photon cross section, $\delta_{\mathrm{TPE}}^{\mathrm{6MAP}}$, for 6MAP it is convenient to ratio the emission of the probe under constant measurement conditions to that for which $\delta_{\mathrm{TPE}}^{\mathrm{S}}$ have been determined (for the standard S). Here, $\delta_{\mathrm{TPE}}^{\mathrm{S}}$, $\Phi_{\mathrm{f}}^{\mathrm{S}}$, and $\Phi_{\mathrm{f}}^{\mathrm{6MAP}}$ are the two-photon cross section for the standard S, the fluorescence quantum yield for S, and the fluorescence

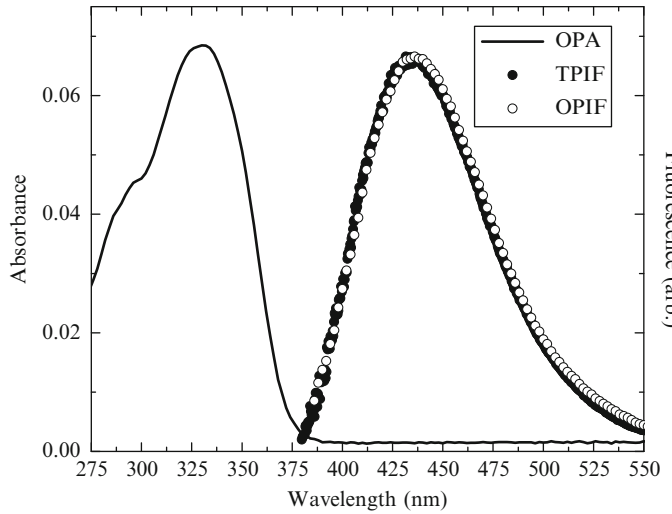

Figure 10.7 One (line)- and two (dots)-photon-induced fluorescence emission spectra of 6MAP in Tris buffer. The one-photon spectrum was taken at a concentration of 20 μM in 6MAP while the two-photon spectrum was obtained at 240 μM. Both spectra have been corrected for the spectral responsivity of the respective spectrometer using quinine sulfate.

quantum yield for 6MAP, respectively. The time-averaged excitation power is assumed to be the same for both measurements. Since the observable is the time-averaged emission intensity $\langle F(t) \rangle$ for the two species, knowledge of the fluorescence quantum yield is necessary to make a quantitative comparison. Xu and Webb (1996) have compiled a table of cross sections for a variety of commonly available laser dyes. Fluorescein was chosen as a standard because its TPE spectrum has been measured with 690 nm excitation.

TPIF emission spectra for both 6MAP and fluorescein (pH 13) were obtained under identical conditions as a function of laser intensity (data not shown). The cross section for TPIF of fluorescein from 690–900 nm has been measured previously and serves as a calibration to determine the cross section of 6MAP (Xu and Webb, 1996). The integrated areas of the emission spectra are compared as described above to obtain $\delta_{\mathrm{TPE}}^{\mathrm{6MAP}} = 0.4(\pm 0.1) \times 10^{-50} \mathrm{cm}^4\mathrm{s/photon}$ (0.4 GM), based on a fluorescence quantum yield of $\Phi_{\mathrm{f}}^{\mathrm{6MAP}} = 0.39$ as measured by Hawkins *et al.* (2001) The cross section was invariant over the range of 50–240 μM. This two-photon cross section is much lower than for most laser dyes, which is consistent with the much more extended π systems of large dye molecules compared to 6MAP. However, the value of $\delta_{\mathrm{TPE}}^{\mathrm{6MAP}}$ for 6MAP is comparable to other fluorophores currently used in two-photon microscopy, such

as dansyl and DAPI (Xu *et al.*, 1996). In addition, the 6MAP two-photon cross section compares favorably with endogenous fluorophores of biological interest such as flavins and nicotinamide (Huang *et al.*, 2002). We therefore expect 6MAP to become a valuable two-photon probe for single molecule studies of DNA dynamics and conformation.

5.9. Single molecule detection of 3MI

Using fluorescence correlation spectroscopy (FCS), it has been found that 3MI is sufficiently bright and stable to be detected at the single molecule level (Sanabia *et al.*, 2004). The use of FCS or single molecule techniques to study the binding and dynamics of DNA is hampered in the UV range by high background fluorescence from many sources of the system including the optics, DNA, coverslip, lens, and other components. FCS measurements yield details such as fluorophore diffusivity, number of fluorophores in the focal volume, intensity, rate of photobleaching, triplet correlation time, triplet fraction, and triplet lifetime (Brand *et al.*, 1997; Dittrich and Schwille, 2001; Eggeling *et al.*, 1998; Thompson, 1991; Zander and Enderlein, 2002). Two parameters that are important indicators for a useful single molecule probe include the count rate per molecule (which must be well above the background count rate) and the photobleaching quantum yield, which when inverted gives the number of photons emitted, on average, before photobleaching occurs. The UV FCS system, based on a homebuilt inverted confocal fluorescence microscope, was developed and used to measure the count rate per molecule, photobleaching quantum yield, and triplet population of 3MI. This system uses an argon laser to obtain continuous wave excitation at 351.1 nm (selected with a BK7 prism) controlled with a half-wave plate followed by a polarizing cube. A telescope and a 50 μm pinhole allowed spatial filtering of the beam with a second telescope to adjust the diameter and convergence entering the objective. To minimize artifacts in analysis the diameter of the laser beam entering the objective was roughly one-half the back-focal plane aperture diameter, underfilling the back aperture (Hess and Webb, 2002). The beam was directed into an inverted oil immersion objective lens (Zeiss Fluar, 1.3 NA, 100×, f = 1.65, infinity corrected) using a dichroic filter (Omega 400DCLP) and measured by a silicon photodiode. Excitation intensities (calculated using power measurements) of samples held in a polydimethylsiloxane (PDMS, Sylgard 184) well on a glass coverslip (Fisher Premium #1) were monitored through a CCD video camera. With 351.1 nm excitation and the 400 nm Raman line blocked using dichroic and band-pass filters, signals passed through a 100 mm focal length achromatic doublet lens and a 50 μm diameter confocal pinhole to a Hamamatsu H7421-40 GaAsP photomultiplier photon-counting detector. Fluorescence intensity of solutions contained in the PDMS well was measured as a function of time with

5 μs resolution. A more detailed account of the theory and data interpretation is presented in the chapter (Sanabia *et al.*, 2004).

In summary, these researchers have shown that single 3MI molecules are detectable using single photon excitation with a signal to background ratio as high as 5, a count rate per molecule above 4 kHz, and a photobleaching quantum yield of 2.4×10^{-4}. The signal from a 3MI-containing oligonucleotide is also detectable on a single molecule level with a signal to background ratio greater than 1. Substantial improvement in both signal to background and photostability are possible with the use of two-photon excitation.

6. Summary

Ideally, a fluorescent nucleoside analog incorporated into an oligonucleotide must be similar enough to native bases to permit native-like behavior of the DNA, but structurally different enough to be highly fluorescent. The electronic configuration within a molecule is the source of its fluorescence. The effect of neighboring bases on the electronic structure of an incorporated pteridine probe and consequently on its fluorescence properties is what allows tracking of structural characteristics of pteridine-containing DNA as it encounters and reacts with other molecules.

We have been unsuccessful at finding a pteridine probe that is more similar to guanine or adenine than those described here. In the initial studies of pteridine probes we found that the two most attractive analogs (probes 5 and 25; Hawkins *et al.*, 1997), essentially 6MI and 6MAP without the 6-position methyl moieties, were extremely unstable. The presence of at least one methyl group in either the 3- or 6-position appears to have a very strong stabilizing effect on these structures. Even with the structural similarities, however, pteridines and purines are electronically quite different. When a fluorescent pteridine molecule is substituted for one of the native bases in the DNA, the overall electronic environment of the DNA molecule is changed. Whether or not this substitution is acceptable to the system under study must be determined experimentally.

The most important features of the pteridine analog probes are that they are unobtrusive enough to be positioned within an oligonucleotide site specifically at or near a location of interest and that they are so intensely fluorescent that they can still be detected within the quenched environment of the oligonucleotide. Early attempts to characterize the properties of pteridine-containing oligonucleotides were focused on the immediate neighbors (two on either side) of the probe. Studies on bulge-forming 3MI sequences (Hawkins, 2003) have revealed that the immediate neighbors to the probe are only a part of the total picture. Strands with the

identical neighboring sequence (AAFAA) but different overall sequences were found to respond quite differently when in a bulged configuration. The entire sequence of bases as well as the overall length and the distance of the probe from each end of the sequence most likely contribute to these variations. Even though subtle differences between sequences may be difficult for researchers to measure, these small variations may be very important to the overall recognition of a strand for physiological function. The incorporated pteridine probes may provide the sensitivity to electronic environment required to detect and understand these subtle variations.

ACKNOWLEDGMENTS

I would like to express my appreciation to the following for generously sharing results of their recent research: Robert J. Stanley and Aiping Yang at Temple University, Philadelphia, PA, for work on the two-photon excitation of 6MAP; Jason Sanabia, Lori Goldner, and Pierre-Antoine Lacaze at National Institutes of Standards and Technology, Gaithersburg, MD for their work on single molecule detection of 3MI; K. Augustyn, K. Wojtuszewski, J. Knutson, and I. Mukerji for the A-tract experiments using 6MAP; and K. Wojtuszewski, Aleksandr Smirnov, and J. Knutsen for the work on time-resolved anisotropies and lifetimes of 36-mers. I especially want to thank Drs. Ishita Mukerji and Jay R. Knutson for helpful discussions.

REFERENCES

Augustyn, K. E., Wojtuszewski, K., Hawkins, M. E., Knutson, J. R., and Mukerji, I. (2006). Examination of the premelting transition of DNA A-tracts using a fluorescent adenosine analogue. *Biochemistry* **45,** 5039–5047.

Berry, D. A., Jung, K.-Y., Wise, D. S., Sercel, A. D., Pearson, W. H., Mackie, H., Randolph, J. B., and Somers, R. L. (2004). Pyrrolo-dC and pyrrolo-C: Fluorescent analogs of cytidine and 2′-deoxycytdine for the study of oligonucleotides. *Tetrahedron Lett.* **45**, 2457–2461.

Brand, L. C. E. O., Zander, C. K. H. D., and Seidel, C. (1997). Single-molecule identification of coumarin-120 by time-resolved fluorescence detection: Comparison of one- and two-photon excitation in solution. *J. Phys. Chem. A* **101,** 4313–4321.

Brand, L., Knutson, J. R., Davenport, L., Beechem, J. B., Dale, R. E., and Kowalczyk, A. A. (1984). Time-resolved fluorescence spectroscopy: Some applications of associative behavior to studies of proteins and membranes. *In* "Dynamics of Molecular Biological Systems" (P. Bayley and R. E. Dale, eds.), 259-305. Academic Press.

Chan, S. S., Breslauer, K. J., Austin, R. H., and Hogan, M. E. (1993). Thermodynamics and premelting conformational changes of phased (dA)5 tracts. *Biochemistry* **29,** 6161–6171.

Chan, S. S., Breslauer, K. J., Hogan, M. E., Kessler, D. J., Austin, R. H., Ojemann, J., Passner, J. M., and Wiles, N. C. (1990). Physical studies of DNA premelting equilibria in duplexes with and without Homo dA*dT tracts: Correlations with DNA bending. *Biochemistry* **29,** 6161–6171.

Crothers, D. M., and Shakked, Z. (1999). DNA bending by adenine-thymine tracts. *In* "Oxford Handbook of Nucleic Acid Structure" (S. Neidle, ed.), pp. 455–470. Oxford University Press, Oxford.

Dash, C., Rausch, J. W., and Le Grice, S. F. (2004). Using pyrrolo-deoxycytosine to probe RNA/DNA hybrids containing the human immunodeficiency virus type-1 3′ polypurine tract. *Nucleic Acids Res.* **32,** 1539–1547.

Davenport, L., Knutson, J. R., and Brand, L. (1986). Faraday Discuss. *Chem. Soc.* **81,** 81–94.

Davis, S. P., Matsumura, M., Williams, A., and Nordlund, T. M. (2003). Position dependence of 2-aminopurine spectra in adenosine pentadeoxynucleotides. *J. Fluorescence* **13,** 249–259.

Dittrich, P. S., and Schwille, P. (2001). Photobleaching and stabilization of fluorophores used for single-molecule analysis with one- and two-photon excitation. *Appl. Phys. B: Lasers Opt.* **73,** 829–837.

Driscoll, S. L., Hawkins, M. E., Balis, F. M., Pfleiderer, W., and Laws, W. R. (1997). Fluorescence properties of a new guanosine analog incorporated into small oligonucleotides. *Biophys. J.* **73,** 3277–3286.

Eckstein, F. (1991). "Oligonucleotides and analogues: A practical approach." *In* "The Practical Approach Series" (D. Rickwood and B. D. Hames, eds.). Oxford University Press, New York.

Eggeling, C. J. W., Rigler, R., and Seidel, C. (1998). Photobleaching of fluorescent dyes under conditions used for single-molecule detection: Evidence of two-step photolysis. *Anal. Chem.* **98,** 10090–10095.

Georghiou, S., Bradrick, T. D., Philippetis, A., and Beechem, J. M. (1996). Large amplitude picosecond anisotropy decay of the intrinsic fluorescence of double stranded DNA. *Biophys. J.* **70,** 1909–1922.

Gokulrangan, G., Unruh, J. R., Holub, D. F., Ingram, B., Johnson, C. K., and Wilson, G. S. (2005). DNA aptamer-based bioanalysis of IgE by fluorescence anisotropy. *Anal. Chem.* **77,** 1963–1970.

Hardman, S. J., and Thompson, K. C. (2006). Influence of base stacking and hydrogen bonding on the fluorescence of 2-aminopurine and pyrrolocytosine in nucleic acids. *Biochemistry* **45,** 9145–9155.

Hawkins, M. E. (2001). Fluorescent pteridine nucleoside analogs: A window on DNA interactions. *Cell Biochem. Biophys.* **34,** 257–281.

Hawkins, M. E. (2003). Fluorescent nucleoside analogues as DNA probes. *In* "DNA Technology" (J. R. Lakowicz, ed.). Vol. 7, pp. 151–175. Kluwer Academic/Plenum Publishers, New York.

Hawkins, M. E., Pfleiderer, W., Balis, F. M., Porter, D., and Knutson, J. R. (1997). Fluorescence properties of pteridine nucleoside analogs as monomers and incorporated into Oligonucleotides. *Anal. Biochem.* **244,** 86–95.

Hawkins, M. E., Pfleiderer, W., Jungmann, O., and Balis, F. M. (2001). Synthesis and fluorescence characterization of pteridine adenosine nucleoside analogs for DNA incorporation. *Analy. Biochem.* **298,** 231–240.

Hawkins, M. E., Pfleiderer, W., Mazumder, A., Pommier, Y. G., and Balis, F. M. (1995). Incorporation of a fluorescent guanosine analog into oligonucleotides and its application to a real time assay for the HIV-1 integrase 3′-processing reaction. *Nucleic Acids Res.* **23,** 2872–2880.

Hawkins, M. E., and Balis, F. M. (2004). Use of pteridine nucleoside analogs as hybridization probes. *Nucleic Acids Res.* **32,** e62.

Heller, C. A., Henry, R. A., McLaughlin, B. A., and Bliss, D. E. (1974). Fluorescence spectra and quantum yields. Quinine, uranine, 9,10-diphenylanthracene, and 9,10-bis (phenylethynyl)anthracenes. *J. Chem. Eng. Data* **19,** 214–219.

Hess, S. T., and Webb, W. W. (2002). Focal volume optics and experimental artifacts in confocal fluorescence correlation spectroscopy. *Biophys. J.* **83,** 2300–2317.

Hill, J. J., and Royer, C. (1997). Fluorescence approaches to study of protein-nucleic acid complexation. *In* ''Methods in Enzymology'' (L. Brand, ed.). Vol. 278, pp. 410–411. Academic Press, New York.

Huang, S., Heikal, A. A., and Webb, W. W. (2002). Two-photon fluorescence spectroscopy and microscopy of NAD(P)H and flavoprotein. *Biophys. J.* **82,** 2811–2825.

Lakowicz, J. R. (1999). ''Principles of Fluorescence Spectroscopy.'' Second edition ed. Plenum Publishers, New York.

Larsen, O. F. A., van Stokkum, I. H. M., Gobets, B., van Grondelle, R., and van Amerongen, H. (2001). Probing the structure and dynamics of a DNA hairpin by ultrafast quenching and fluorescence depolarization. *Biophys. J.* **81,** 1115–1126.

Lee, B. J., Barch, M., Castner, E. W., Jr., Volker, J., and Breslauer, K. J. (2007). Structure and dynamics in DNA looped domains: CAG triplet repeat sequence dynamics probed by 2-AMinopurine fluorescence. *Biochemistry* **46,** 10756–10766.

Liu, C., and Martin, C. T. (2001). Fluorescence characterization of the transcription bubble in elongation complexes of T7 RNA polymerase. *J. Mol. Biol.* **308,** 465–475.

Mukerji, I., and Williams, A. P. (2002). UV resonance raman and circular dichroism studies of a DNA duplex containing an A(3)T(3) tract: Evidence for a premelting transition and three-centered H-bonds. *Biochemistry* **41,** 69–77.

Myers, J. C., Moore, S. A., and Shamoo, Y. (2003). Structure-based incorporation of 6-methyl-8-(2-deoxy-beta-ribofuranosyl)isoxanthopteridine into the human telomeric repeat DNA as a probe for UP1 binding and destabilization of G-tetrad structures. *J. Biol. Chem.* **278,** 42300–42306.

Nordlund, T. M., Andersson, S., Nilsson, L., Rigler, R., Graslund, A., and McLaughlin, L. W. (1989). Structure and dynamics of a fluorescent DNA oligomer containing the EcoRI recognition sequence: Fluorescence, molecular dynamics, and NMR studies. *Biochemistry* **28,** 9095–9103.

Ou, C. Y., Kwok, S., Mitchell, S. W., Mack, D. H., Sninsky, J. J., Krebs, J. W., Feorino, P., Warfield, D., and Schochetman, G. (1988). DNA amplification for direct detection of HIV-1 in DNA of peripheral blood mononuclear cells. *Science* **239,** 295–297.

Park, Y.-W., and Breslauer, K. J. (1991). A spectroscopic and calorimetric study of the melting behaviors of a 'bent' and 'normal' DNA duplex: [d(GA4T4C)]2 versus [d(GT4A4C)]2. *Proc. Natl. Acad. Sci. USA* **88,** 1551–1555.

Rai, P., Cole, T. D., Thompson, E., Millar, D. P., and Linn, S. (2003). Steady-state and time-resolved fluorescence studies indicate an unusual conformation of 2-aminopurine within ATAT and TATA duplex DNA sequences. *Nucleic Acids Res.* **31,** 2323–2332.

Ramreddy, T., Rao, B. J., and Krishnamoorthy, G. (2007). Site-specific dynamics of strands in ss- and dsDNA as revealed by time-domain fluorescence of 2-aminopurine. *J. Phys. Chem. B* **111,** 5757–5766.

Rist, M. J., and Marino, J. P. (2002). Fluorescent nucleotide base analogs as probes of nucleic acid structure, dynamics and interactions. *Curr. Org. Chem.* **6,** 775–793.

Sanabia, J. E., Goldner, L. S., Lacaze, P-A., and Hawkins, M. E. (2004). On the feasibility of single-molecule detection of the guanosine-analogue 3-MI. *J. Phys. Chem. B* **108,** 15293–15300.

Schurr, J. M., and Fujimoto, B. S. (1988). The amplitute of local angular motions of intercalated dyes and bases in DNA. *Biopolymers* **27,** 1543–1569.

Seibert, E., Chin, A. S., Pfleiderer, W., Hawkins, M. E., Laws, W. R., Osman, R., and Ross, J. B. A. (2003). pH-dependent spectroscopy and electronic structure of the guanine analogue 6,8-Dimethylisoxanthopterin. *J. Phys. Chem. A* **107,** 178–185.

Sischka, A., Toensing, K., Eckel, R., Wilking, S. D., Sewald, N., Ros, R., and Anselmetti, D. (2005). Molecular mechanisms and kinetics between DNA and DNA binding lignands. *Biophys. J.* **88,** 404–411.

Stanley, R. J., Hou, Z., Yang, A., and Hawkins, M. E. (2005). The two-photon excitation cross section of 6MAP, a fluorescent adenine analogue. *J. Phys. Chem. B* **109,** 3690–3695.

Tanaka, M., Srinivas, R. V., Ueno, T., Kavlick, M. F., Hui, F. K., Fridland, A., Driscoll, J. S., and Mitsuya, H. (1997). *In vitro* induction of human immunodeficiency virus type 1 variants resistant to 2′-beta-Fluoro-2′,3′-dideoxyadenosine. *Antimicrob. Agents Chemother.* **41,** 1313–1318.

Thompson, N. L. (1991). Fluorescence correlation spectroscopy. *In* ''Topics in Fluorescence Spectroscopy'' (J. R. Lakowicz, ed.), **1,** p. 337. Plenum Press, New York.

Unruh, J. R., Gokulrangan, G., Lushington, G. H., Johnson, C. K., and Wilson, G. S. (2005a). Orientational dynamics and dye-DNA interactions in a dye-labeled DNA aptamer. *Biophys. J.* **88,** 3455–3465.

Unruh, J. R., Gokulrangan, G., Wilson, G. S., and Johnson, C. K. (2005b). Fluorescence properties of fluorescein, tetramethylrhodamine and texas red linked to a DNA aptamer. *Photochem. Photobiol.* **81,** 682–690.

Vamosi, G., Gohlke, C., and Clegg, R. M. (1996). Fluorescence characteristics of 5-carboxytetramethylrhodamine linked covalently to the 5′ end of oligonucleotides: Multiple conformers of single-stranded and double-stranded dye-DNA complexes. *Biophys. J.* **71,** 972–994.

Wiegand, T. W., Williams, P., Dreskin, S. C., Jouvin, M.-H., Kinet, J.-P., and Tasset, D. (1996). High-affinity oligonucleotide ligands to human IgE inhibit binding to Fcε receptor I. *J. Immunol.* **157,** 221–230.

Wojtuszewski, K., Hawkins, M., Cole, J. L., and Mukerji, I. (2001). HU binding to DNA: Evidence for multiple complex formation and DNA bending. *Biochemistry* **40,** 2588–2598.

Xu, C., and Webb, W. W. (1996). Measurement of two-photon excitation cross sections of molecular fluorphores with data from 690 to 1050 nm. *J. Opt. Soci. Am. B: Opt. Phys.* **13,** 481–491.

Xu, C., Willliams, R. M., Zipfel, W., and Webb, W. W. (1996). Multiphoton excitation cross-sections of molecular fluorophores. *Bioimaging* **4,** 198–207.

Xu, Y., and Sugiyama, H. (2006). Formation of the G-quadruplex and i-motif structures in retinoblastoma susceptibility genes (Rb). *Nucleic Acids Res.* **34,** 949–954.

Zander, C., and Enderlein, J. (2002). *In* ''Single Molecule Detection in Solution, Methods and Applications'' (R. A. Keller, ed.). Wiley-VCH, Berlin.